Low-noise wideband ultrasound detection using polymer microring resonators

Sheng-Wen Huang,[1] Sung-Liang Chen,[2] Tao Ling,[2] Adam Maxwell,[2] Matthew O'Donnell,[3] L. Jay Guo,[2,a)] and Shai Ashkenazi[1,b)]
[1]*Department of Biomedical Engineering, University of Michigan, Ann Arbor, Michigan 48109, USA*
[2]*Department of Electrical Engineering and Computer Science, University of Michigan, Ann Arbor, Michigan 48109, USA*
[3]*Department of Bioengineering, University of Washington, Seattle, Washington 98195, USA*

(Received 27 February 2008; accepted 24 April 2008; published online 15 May 2008)

Polymer microring resonators for low-noise, wideband ultrasound detection are presented. Using a nanoimprinting technique, we fabricated polymer microring resonators with a quality factor of 6000 resulting in high sensitivity to ultrasound. A noise-equivalent pressure of 0.23 kPa over 1–75 MHz and a detection bandwidth of over 90 MHz at −3 dB were measured. These results demonstrate the potential of polymer microring resonators for high-frequency ultrasound and photoacoustic imaging. For a typical photoacoustic imaging test case, the high sensitivity demonstrated in these devices would increase imaging depth by a factor of 3 compared to state-of-the-art polyvinylidene fluoride detectors. © *2008 American Institute of Physics*. [DOI: 10.1063/1.2929379]

In ultrasound (pulse-echo) and photoacoustic (also called optoacoustic) imaging, high resolution is achieved using high frequencies above 20 MHz. High-frequency ultrasound imaging has been applied to intravascular imaging,[1] endosonography,[2] small animal imaging,[3] skin imaging,[4] and ophthalmology.[5] Biomedical applications of high-frequency photoacoustic imaging include microvasculature visualization,[6] functional imaging,[7] and intravascular imaging.[8] In all these works, piezoelectric transducers were used.

Small element size and spacing and large element count are essential for high resolution three-dimensional (3D) imaging. Two-dimensional (2D) arrays are required for high frame rate 3D ultrasound and photoacoustic imaging. However, the realization of such arrays using piezoelectric technology is highly restricted due to increased noise level in small elements, complexity of electrical interconnects, and fabrication difficulties. One way to avoid these difficulties is to detect and generate ultrasound optically.[9]

Resonant optical ultrasound transducers (ROUTs) have been studied for decades.[9–19] Their advantages include immunity against electromagnetic interference, easier realization of large and dense arrays with element sizes of 10–100 μm, high acoustic bandwidth, and element signal-to-noise ratio (SNR) primarily dependent on optical probing power rather than detector size. In this letter, we focus on a ROUT platform incorporating polymer microring resonator sensor, polymer resonator for optical ultrasound detection (PROUD).[13,18,19] Specifically, low noise-equivalent pressure (NEP) and wide detection bandwidth of PROUD are demonstrated.

A microring resonator consists of a ring waveguide closely coupled with a bus waveguide which serves as light input and output. When the round-trip phase acquired by the guided wave in the ring is equal to $2m\pi$, where m is an integer, the field of the optical wave returning to the coupler from the ring is in antiphase with the optical wave traveling through the bus waveguide, resulting in a resonance dip in the transmission spectrum. In the presence of ultrasound, acoustic pressure deforms the waveguide dimensions and changes the refractive index of the polymer via the elasto-optic effect,[20] and consequently modulates the round-trip phase acquired by the guided wave in the ring, leading to a shift of the resonance wavelength.[18] At a fixed wavelength with a high slope in the transmission spectrum (i.e., around a resonance dip), the phase modulation is transformed into amplitude modulation of the output power with high gain, and ultrasound detection is realized by detecting the optical output power. High quality (Q) factor leads, therefore, to high sensitivity.

We fabricated PROUD devices on 500 μm thick silicon substrates using a nanoimprinting technique.[21] They operate at optical wavelengths around 1550 nm with polymer waveguides 2×2 μm^2 in cross section. The microrings used in the following experiments have a 100 μm diameter. Optical fibers were butt coupled to the input and output of its bus waveguide using UV curable epoxy (Loctite 3526, Henkel Loctite Corp., Rocky Hill, CT) mounting. To provide better mode matching, a 10.5 μm mode-field-diameter single-mode fiber was first spliced to a 4.8 μm mode-field-diameter fiber, which was then connected to the bus input to maximize the amount of light coupled into the polymer waveguide. A multimode fiber with a 62.5 μm core diameter was aligned with the output of the waveguide.

The setup shown in Fig. 1 was used to measure the NEP and sensitivity of a PROUD device. A continuous-wave tunable laser source (HP 8168F, Agilent Technologies, Santa

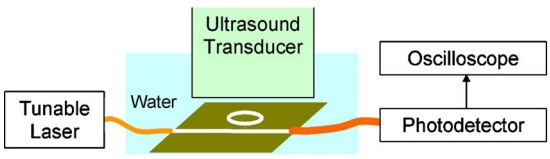

FIG. 1. (Color online) Experimental setup to measure the NEP and the sensitivity of a polymer microring resonator. The distance between the ultrasound transducer and the resonator was 1.5 mm.

a)Electronic mail: guo@umich.edu.
b)Electronic mail: shaia@umich.edu.

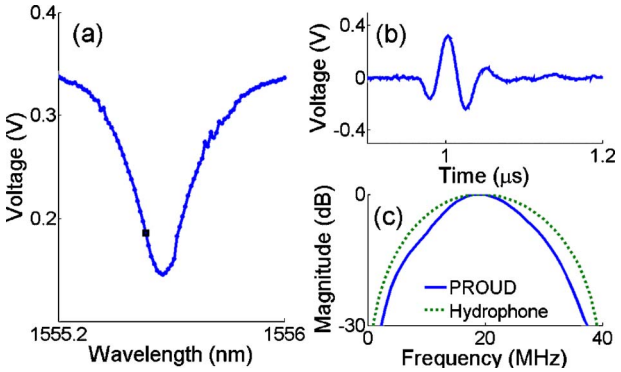

FIG. 2. (Color online) (a) Optical transmission spectrum of a polymer microring resonator. The input power was 4.2 mW. The resonance wavelength and the bandwidth were 1555.57 and 0.24 nm, respectively. (b) Single-shot acoustic waveform measured by the resonator. The positive peak corresponds to 30 kPa. The optical probing wavelength and input power were set to 1555.51 nm [indicated with a square in (a)] and 5.5 mW, respectively. (c) Spectra of acoustic waveforms measured by the resonator and a hydrophone.

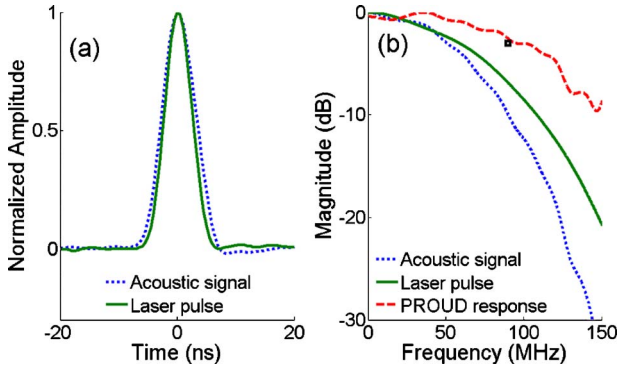

FIG. 3. (Color online) (a) Acoustic signal detected by a polymer microring resonator and laser pulse profile detected by the photodetector. (b) Spectra of the signals and frequency response of the resonator. A square indicating (90 MHz, −3 dB) is shown as a reference. The detection bandwidth of the resonator is over 90 MHz at −3 dB.

Clara, CA) was connected to the device's input fiber, and the output fiber was connected to a photodetector (1811-FC, New Focus, San Jose, CA), which has a dc output gain of 1 V/A and ac output gain of 4×10^4 V/A with an electrical bandwidth of 25 kHz–125 MHz. The photodetector output to a digital oscilloscope (WaveSurfer 432, LeCroy, Chestnut Ridge, NY) for data collection.

Using the dc output, we measured the device's transmission spectrum, shown in Fig. 2(a), with an input power of 4.2 mW. The Q factor was estimated to be ~6000. The off-resonance light transmission shows that only 9% of the probing light was collected by the photodetector mainly due to mode mismatch at the fiber-waveguide coupling region. The ratio can be improved with optimized device design and fabrication.

A 20 MHz unfocused transducer (V316, Panametrics NDT, Waltham, MA) with a 3.18 mm diameter was used to insonify the microring. It outputs a peak pressure of 30 kPa around its surface, calibrated using a hydrophone,[19] when driven by a 10 V peak-to-peak one-cycle 20 MHz sinusoidal wave. The acoustic coupling medium was de-ionized water. The optical probing wavelength and input power were set to 1555.51 nm and 5.5 mW, respectively. Ultrasound signals were detected by the ac output of the photodetector.

Figure 2(b) shows a recorded signal trace and Fig. 2(c) shows the spectra of the signal and an acoustic waveform measured by the hydrophone. The ringing waveform following the main pulse signal was due to reflections within the silicon substrate, which can be removed by changing substrate materials and/or structures. Since a 30 kPa acoustic pressure produced an output voltage of 332 mV, the sensitivity of the PROUD device was 11 mV/kPa. The root-mean-square noise levels were 1.5, 2.2, and 2.5 mV over 1–25, 1–50, and 1–75 MHz bandwidths, respectively, and the corresponding NEPs, a measure of the minimum detectable pressure of the device, were 0.14, 0.20, and 0.23 kPa [=(2.5 mV)/(11 mV/kPa)] by extrapolating the sensitivity to higher frequencies. The extrapolation is valid since all the bands are well below the −3 dB detection bandwidth of the device. Compared to the previous best result, 4.1 kPa over 5–75 MHz,[19] we have improved NEP by more than one order of magnitude. The same level of NEP was achieved using a Fabry–Pérot ROUT with a detection bandwidth of 20 MHz and a detector diameter of 50 μm.[17] The PROUD device is 20 times more sensitive than a 75 μm piezoelectric polyvinylidene fluoride (PVDF) transducer (HPM075/1, Precision Acoustics, Dorchester, Dorset, UK; http://www.acoustics.co.uk/products/hpm075-1), which has an NEP lower bound of 6 kPa [=(60 μV)/(10 nV/Pa)] over a 100 MHz bandwidth considering only the noise from its matched preamplifier (HP1, Precision Acoustics). In addition, PROUD's NEP can be further reduced by coupling more detection light into a device or by increasing its Q factor.

A wideband optoacoustic source was utilized to measure the detection bandwidth of a PROUD device. A 100 nm thick chromium film was deposited onto a glass substrate. Illuminating such a film with a wide-spot nanosecond laser pulse generates a planar acoustic wave with a temporal profile duplicating that of the excitation laser pulse shape.[22,23] The chromium film was placed 540 μm from a PROUD device and was illuminated by a 532 nm pulsed frequency-doubled Nd-YAG (yttrium aluminum garnet) laser (Surelite I-20, Continuum, Santa Clara, CA) with a spot size of 4.5 mm in diameter. The acoustic coupling medium was de-ionized water. An acoustic pulse signal detected by the PROUD device and a laser pulse profile detected directly by the same photodetector are shown in Fig. 3(a). Figure 3(b) presents corresponding spectra together with the estimated frequency response of the device, obtained by taking the difference of the two spectra and compensating for acoustic attenuation in water assuming an attenuation coefficient of 2.2×10^{-4} dB/cm MHz^2.[24] The detection bandwidth of the PROUD device was over 90 MHz at −3 dB. As a reference, limited by equipment, we could only confirm a detection bandwidth of 55 MHz previously.[18] Theoretically, the bandwidth can be estimated as the frequency at which the corresponding quarter wavelength is equal to the thickness of the polymer waveguide. In this way, the response is expected to roll off at 300 MHz. To be able to measure a detection bandwidth of hundreds of megahertz, a more wideband photodetector and a more uniform and wideband planar wave are required.

PROUD's high sensitivity and wide bandwidth make it an excellent candidate for 3D photoacoustic imaging, where dense 2D arrays are required for detection of relatively low laser-generated acoustic signals with high image contrast. Wide bandwidth improves image resolution in both ultra-

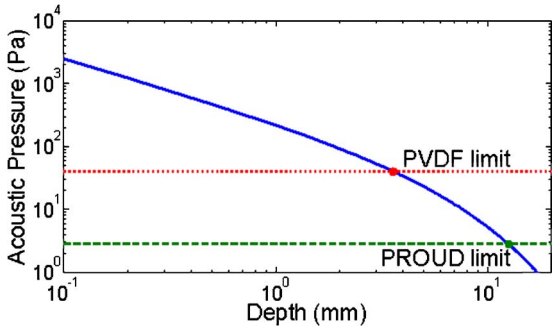

FIG. 4. (Color online) Acoustic pressure generated by laser absorption in a 100 μm bloodlike object embedded in tissue, as a function of tissue depth. The dotted line represents the detection limit using a PVDF piezoelectric detector array, and the dashed line represents the detection limit of a PROUD array. No averaging is assumed except coherent summation over 2500 array elements. Laser fluence is 20 mJ/cm^2.

sound and photoacoustic imaging. Furthermore, the flat spectral response from dc to high frequencies is particularly beneficial in photoacoustic imaging. In ultrasound imaging, contrast between tissues is established by their different levels of inhomogeneity at scales comparable to the ultrasound wavelength. Large scale objects are therefore probed by their fine structure properties. On the other hand, photoacoustic image reconstruction of multiscale anatomical structures relies on sound generated at a wide bandwidth with acoustic wavelengths corresponding to the various scales of the object. PROUD's flat response from dc to 90 MHz provides a unique advantage for photoacoustic imaging.

Typically photoacoustic signals are 20 to 40 dB weaker than the ultrasound signals used in medical imaging. The high sensitivity of a PROUD device can be translated into deeper penetration for photoacoustic imaging. To quantify the expected improvement in imaging depth using a PROUD as compared to a piezoelectric detector, we analyze a case of photoacoustic detection of a small object. Assuming a frequency range of 0–20 MHz and a 2D array of 50×50 devices, the effective NEP is 2.8 Pa using PROUD and 40 Pa using similar size PVDF piezoelectric detectors. Consider a 100 μm bloodlike water-based object with an effective optical absorption coefficient of $\mu_{\text{eff}}^{\text{blood}}=5$ cm^{-1} (typical for blood at 800 nm wavelength) embedded in a normal water-based tissue with an effective optical absorption coefficient of $\mu_{\text{eff}}^{\text{tissue}}=1$ cm^{-1}. The peak acoustic pressure at the detector surface, generated by light absorption in the object at a depth z, is given by[25]

$$P=\frac{R}{z}\times\frac{c^2\beta(\mu_{\text{eff}}^{\text{blood}}-\mu_{\text{eff}}^{\text{tissue}})J_0}{2C_P}\times\exp(-\mu_{\text{eff}}^{\text{tissue}}z)\times 10^{-Az/20},$$

where $J_0=20$ mJ/cm^2 is the surface optical fluence, $R=50$ μm is the object radius, $c=1500$ m/s is the sound speed, $\beta=360\times 10^{-6}$ K^{-1} is the thermal expansion coefficient,[26] $C_P=4.2$ kJ/kg K is the specific heat capacity, and $A=5$ dB/cm is the ultrasound attenuation in the tissue. The resulting acoustic pressure as a function of the object's depth is shown in Fig. 4. Imaging depths (defined by unit SNR) obtained using PROUD and PVDF detector arrays are 12.6 and 3.6 mm, respectively. The depth improvement gained by using PROUD is over threefold.

To form a dense and large element-count 2D array with PROUD devices, wavelength multiplexing techniques can be used, which could drastically reduce the number of input/output leads to address the elements. We already experimentally confirmed the feasibility of using a single bus waveguide to address four ring elements.[19] An M by N detection array may have M buses with each one shared by N rings and M N-channel demultiplexers to allow all channels to work in parallel.[18] Our current PROUD devices have limited angular sensitivity at high frequencies due to their large diameters. By designing rings to operate in the visible wavelength range, microrings with a diameter on the order of 15–20 μm can be realized in theory. Smaller rings provide better angular sensitivity and enable more rings to share the same bus. Combining PROUD devices with optoacoustic transmitters such as a gold nanostruture[9] to enable ultrasound imaging is also part of the future work.

Support from NIH Grant No. EB007619-01A1 and NSF Grant No. CBET 0730446 are gratefully acknowledged.

[1] R. A. White, C. E. Donayre, G. E. Kopchok, I. Walot, C. M. Mehinger, E. P. Wilson, and C. deVirgilio, World J. Surg. **20**, 622 (1996).
[2] A. Chak, Endoscopy **32**, 146 (2000).
[3] F. S. Foster, M. Y. Zhang, Y. Q. Zhou, G. Liu, J. Mehi, E. Cherin, K. A. Harasiewicz, B. G. Starkoski, L. Zan, D. A. Knapik, and S. L. Adamson, Ultrasound Med. Biol. **28**, 1165 (2002).
[4] M. Vogt, K. Kaspar, P. Altmeyer, K. Hoffmann, and S. El Gammal, Frequenz **55**, 12 (2001).
[5] D. J. Coleman, R. H. Silverman, A. Chabi, M. J. Rondeau, K. K. Shung, J. Cannata, and H. Lincoff, Ophthalmology **111**, 1344 (2004).
[6] R. J. Zemp, R. Bitton, M.-L. Li, K. K. Shung, G. Stoica, and L. V. Wang, J. Biomed. Opt. **12**, 010501 (2007).
[7] H. F. Zhang, K. Maslov, M. Sivaramakrishnan, G. Stoica, and L. V. Wang, Appl. Phys. Lett. **90**, 053901 (2007).
[8] S. Sethuraman, J. H. Amirian, S. H. Litovsky, R. W. Smalling, and S. Y. Emelianov, Opt. Express **15**, 16657 (2007).
[9] Y. Hou, J.-S. Kim, S. Ashkenazi, S.-W. Huang, L. J. Guo, and M. O'Donnell, Appl. Phys. Lett. **91**, 073507 (2007).
[10] J.-P. Monchalin, Appl. Phys. Lett. **47**, 14 (1985).
[11] J. D. Hamilton, T. Buma, M. Spisar, and M. O'Donnell, IEEE Trans. Ultrason. Ferroelectr. Freq. Control **47**, 160 (2000).
[12] V. Wilkens, J. Acoust. Soc. Am. **113**, 1431 (2003).
[13] S. Ashkenazi, C.-Y. Chao, L. J. Guo, and M. O'Donnell, Appl. Phys. Lett. **85**, 5418 (2004).
[14] S. Ashkenazi, Y. Hou, T. Buma, and M. O'Donnell, Appl. Phys. Lett. **86**, 134102 (2005).
[15] M. Klann and C. Koch, IEEE Trans. Ultrason. Ferroelectr. Freq. Control **52**, 1546 (2005).
[16] E. Zhang and P. Beard, IEEE Trans. Ultrason. Ferroelectr. Freq. Control **53**, 1330 (2006).
[17] E. Z. Y. Zhang and P. Beard, Proc. SPIE **5320**, 222 (2004).
[18] C.-Y. Chao, S. Ashkenazi, S.-W. Huang, M. O'Donnell, and L. J. Guo, IEEE Trans. Ultrason. Ferroelectr. Freq. Control **54**, 957 (2007).
[19] A. Maxwell, S.-W. Huang, T. Ling, J.-S. Kim, S. Ashkenazi, and L. J. Guo, IEEE J. Sel. Top. Quantum Electron. **14**, 191 (2008).
[20] K. Okamoto, *Fundamentals of Optical Waveguides* (Academic, San Diego, 2000).
[21] C.-Y. Chao and L. J. Guo, J. Vac. Sci. Technol. B **20**, 2862 (2002).
[22] G. J. Diebold, T. Sun, and M. I. Khan, Phys. Rev. Lett. **67**, 3384 (1991).
[23] T. Buma, M. Spisar, and M. O'Donnell, Proc.-IEEE Ultrason. Symp. **2**, 1253 (1999).
[24] J. M. Cannata, J. A. Williams, Q. Zhou, T. A. Ritter, and K. K. Shung, IEEE Trans. Ultrason. Ferroelectr. Freq. Control **53**, 224 (2006).
[25] A. A. Oraevsky and A. A. Karabutov, Proc. SPIE **3916**, 228 (2000).
[26] G. Elert, *The Physics Hypertextbook* (http://hypertextbook.com/physics/thermal/expansion/).